Structure and electrical conductance of Pb-covered Si(111) surfaces

Xiao Tong* and Kotaro Horikoshi
Department of Physics, School of Science, University of Tokyo, Hongo 7-3-1, Bunkyo-ku, Tokyo 113-0033, Japan

Shuji Hasegawa
Department of Physics, School of Science, University of Tokyo, Hongo 7-3-1, Bunkyo-ku, Tokyo 113-0033, Japan
and Core Research for Evolutional Science and Technology (CREST), The Japan Science and Technology Corporation (JST), Kawaguchi Center Building, Hon-cho 4-1-8, Kawaguchi, Saitama 332-0012, Japan

(Received 13 August 1998; revised manuscript received 30 April 1999)

A dense commensurate $\sqrt{3}\times\sqrt{3}$ phase was obtained by additional 0.7 ML Pb adsorption onto the Si(111)-$\sqrt{3}\times\sqrt{3}$-Pb surface ($\frac{1}{3}$ ML Pb) at room temperature (RT). Its electronic structure was similar to that of the hexagonal and striped incommensurate (HIC and SIC) phases. A high surface electrical conductance observed for this phase was attributed partly to an increase of carrier concentration in the surface space-charge layer, and more importantly to the formation of a metallic surface state. The HIC phase, on the other hand, was found to convert to the SIC phase with only 0.08 ML additional Pb adsorption at RT, which was accompanied with a steep increase in conductance. This was due to an increase of carrier concentration in the metallic surface state, and also possibly due to an enhancement of its carrier mobility. Both enhancements are suggested to come from the reduced domain-wall density in the SIC phase compared with the HIC phase.
[S0163-1829(99)09731-3]

I. INTRODUCTION

The surface states are localized only near the topmost atomic layers, which provide an inherently two-dimensional electron system, and are expected to have novel properties correlating with surface-structural modifications on atomic scales. We have reported that $\sqrt{21}\times\sqrt{21}$ superstructures on Si(111) have highly conductive surface-state bands.[1–4] However, the surface-state conductance is expected to be influenced by extrinsic structural defects on surfaces such as steps and domain boundaries. So it will be interesting to investigate the relation between the surface defects and the electronic transport properties of surface-state bands.

In this context, we have chosen Pb-adsorbed Si(111) surfaces for two reasons. First, it has been reported that only submonolayer Pb adsorption is enough to metallize the Si surface,[5,6] which will enable us to detect the excess electrical conductance through the metallic surface-state bands (or through the topmost metal atomic layers). Second, the Pb/Si(111) surface is known to exhibit various phases depending on Pb coverage. Especially, characteristic distributions of domain boundaries are formed in its incommensurate phases. In these phases, small domains of a commensurate $\sqrt{3}\times\sqrt{3}$ structure, which is described by a close-packed 30° rotated Pb(111) layer on a bulk-terminated Si(111) surface, are separated by a large quantity of domain walls.[7,8] So we expect to have an opportunity to detect some effects of the domain boundaries on the electrical conductance through the Pb adlayers.

Some studies about electrical conduction on the Si(111) surfaces upon deposition of Pb adlayers have been presented. Oscillatory changes in conductance were found during growth of Pb atomic layers,[9] which were interpreted in terms of quantum size effects on the conductance through the Pb layers. Suurmeijer *et al.* measured the electrical conductance of a Si(111)-7×7 surface upon epitaxial Pb adsorption up to a few ML,[5] and suggested a formation of a metallic phase only with submonolayer Pb adsorption.

In the present study, we have chosen two phases on Pb/Si(111) surfaces as starting substrates, the $\sqrt{3}\times\sqrt{3}$ phase with $\frac{1}{3}$ ML Pb (Refs. 10 and 11) and the hexagonal incommensurate (HIC) phase near 1 ML Pb coverage.[7,8] By depositing additional Pb onto these surfaces at RT, we have observed structural changes using reflection high-energy electron diffraction (RHEED), electronic structures by photoemission spectroscopies, and simultaneously measured the electrical conductance changes.

II. EXPERIMENTS

The experiments were carried out in an ultrahigh vacuum multichamber whose base pressure was lower than 5×10^{-10} Torr. It consisted of a RHEED system, an x-ray source ($\mathrm{Mg}\,K\alpha$), an ultraviolet (UV) light source ($\mathrm{He}\,I$), an electron analyzer (VG ADES 500) (Ref. 4), and a sample holder for four-probe electrical conductance measurements.[12] A *p*-type Si(111) wafer with nominal resistivity of 20 Ω cm was cleaned by repeated flash heating at 1500 K to obtain the clean Si(111)-7×7 surface. After depositing about 1.3 ML Pb onto the 7×7 surface at RT (monolayer equals 7.8×10^{14} atoms/cm^2), the substrate was subsequently heated up to about 570 K for a few seconds, and then cooled down to RT. Then, the hexagonal incommensurate phase was obtained. With further annealing, e.g., 1 min at 570 K, the $\sqrt{3}\times\sqrt{3}$-Pb phase with Pb coverage of $\frac{1}{3}$ ML was produced. This is because some Pb atoms thermally desorb from the surface. The Pb deposition rate was measured with a crystal oscillator.

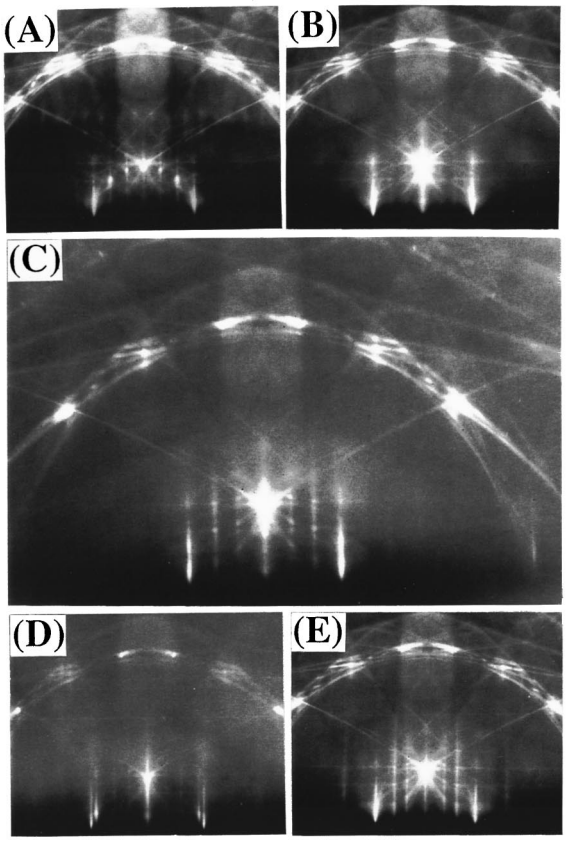

FIG. 1. A series of RHEED patterns taken during additional Pb deposition at RT onto the Si(111)-$\sqrt{3}\times\sqrt{3}$-Pb surface of $\frac{1}{3}$ ML Pb coverage. (A) The initial $\sqrt{3}\times\sqrt{3}$-Pb surface, (B) the 1×1-Pb phase, (C) the dense commensurate $\sqrt{3}\times\sqrt{3}$-Pb phase, and (D) the dense commensurate $\sqrt{3}\times\sqrt{3}$-Pb phase with Pb crystal islands on it, respectively. (E) The HIC-phase pattern is shown for comparison.

III. RESULTS AND DISCUSSIONS

A. On the $\sqrt{3}\times\sqrt{3}$-Pb surface

Figure 1 shows the changes in RHEED pattern during additional Pb deposition onto the $\sqrt{3}\times\sqrt{3}$-Pb surface ($\frac{1}{3}$ ML) at RT. The initial $\sqrt{3}\times\sqrt{3}$ phase (A) was converted gradually into a 1×1 phase mixed with very weak streaks of the $\sqrt{3}\times\sqrt{3}$ fractional order (B) around 0.46 ML coverage [for brevity, we call (B) a 1×1 phase hereafter]. Then the intensity of the $\sqrt{3}\times\sqrt{3}$ streaks increased and became the sharpest around 0.7 ML coverage as shown in (C). Beyond 0.7 ML Pb crystals grew as indicated by streaks appearing outside the Si fundamental spots on the zeroth Laue zone in (D), which correspond to a Pb lattice constant. The RHEED pattern (C) is different from those of the reported dilute commensurate $\sqrt{3}\times\sqrt{3}$ structures such as that at $\frac{1}{3}$ ML Pb [see (A)] and the mosaic phase at $\frac{1}{6}$ ML coverage,[10,11] and dense incommensurate [HIC and striped incommensurate SIC] phases as shown in Fig. 1(E) and Fig. 5(F). By carefully comparing (E) and (C), one will notice that the horizontal spacings among the $\sqrt{3}\times\sqrt{3}$ fractional-order streaks and the fundamental streaks on the zeroth Laue zone are different;[10,13] they are equidistant in (C), while they are not in (E). Therefore we have discerned that the phase (C) is a dense commensurate $\sqrt{3}\times\sqrt{3}$ phase (total Pb coverage is 1.0 ML), which was not reported before.

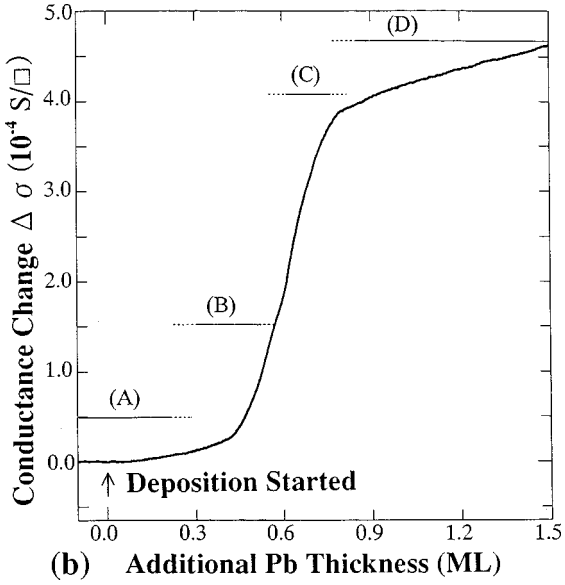

FIG. 2. Change of conductance of a Si wafer during the Pb deposition onto the Si(111)-$\sqrt{3}\times\sqrt{3}$-Pb ($\frac{1}{3}$ ML) surface at RT. The RHEED patterns shown in Fig. 1 are also indicated at the corresponding coverage ranges, which were observed in the separate runs of depositions under the same conditions.

Figure 2 shows the changes in electrical conductance of the Si wafer during the structural changes mentioned above by Pb deposition. The RHEED patterns shown in Fig. 1 are also indicated at the corresponding coverages. With the transformation from the initial $\sqrt{3}\times\sqrt{3}$-Pb phase (A) into the 1×1 structure (B), the conductance increased gradually, then it began to rise steeply when the phase (B) changed into the dense commensurate $\sqrt{3}\times\sqrt{3}$ phase (C). The steep conductance increase ceased around 0.7 ML coverage where the pattern (D) began to appear. The conductance continued to increase slowly with further deposition. In this way, the phase (C) seems to make the surface highly conductive.

Figure 3 shows the normal-emission ultraviolet photoemission spectra taken from the clean 7×7 surface, $\sqrt{3}\times\sqrt{3}$ ($\frac{1}{3}$ ML) phase (A), 1×1 phase (B), dense commensurate $\sqrt{3}\times\sqrt{3}$ phase (C), and the phase (D). In these spectra, one will notice two features; the first is the emission intensity at E_F. For the phase (A), no distinct emission is observed at E_F, while during the successive structural transformation (B)→(C)→(D), the observable emission intensities at E_F appear and become stronger. Another point is that the prominent bulk-emission peak at 1.8 eV below E_F for the clean 7×7 surface[14] is shifted by about (A) 0.05 ± 0.05 eV, (B) 0.50 ± 0.07 eV, and (C) 0.45 ± 0.08 eV towards E_F, respectively, as indicated by arrows. Weitering, Ettema, and Hibma[15] also found that this bulk-state peak shifted towards E_F by 0.55 eV during the transformation from the clean 7×7 surface into the incommensurate phase (HIC or SIC). They concluded that this shift was solely due to band bending and that possible hybridization effects were negligible. By using the fundamental parameters that the E_F positions at the clean 7×7 surface and in bulk are located at 0.63 and 0.29 eV above the valence-band maximum (VBM),[16] respectively, in our samples, and that the bulk band gap is 1.12 eV, it is obtained that the E_F positions at the respective phases are (A) 0.58 ± 0.05 eV, (B) 0.13 ± 0.07 eV, and (C) 0.18

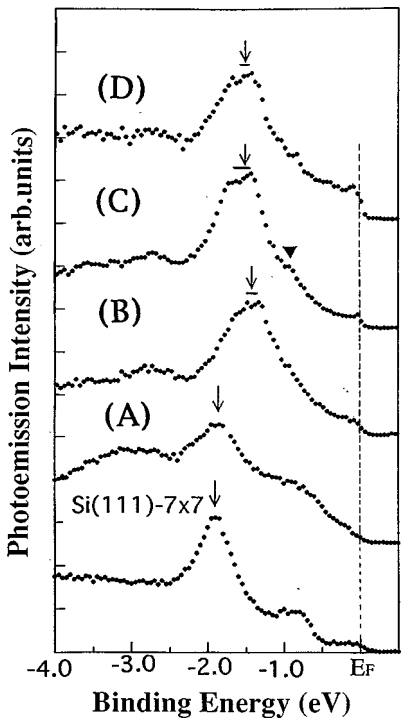

FIG. 3. Normal-emission UPS spectra taken from the clean Si(111)-7×7 surface, (A) the $\sqrt{3}\times\sqrt{3}$-Pb ($\frac{1}{3}$ ML) phase, (B) the 1×1, (C) the dense commensurate $\sqrt{3}\times\sqrt{3}$-Pb (1 ML) phase, and (D) the dense commensurate $\sqrt{3}\times\sqrt{3}$-Pb (1 ML) phase with Pb crystal islands on it, respectively, corresponding to the RHEED patterns shown in Fig. 1.

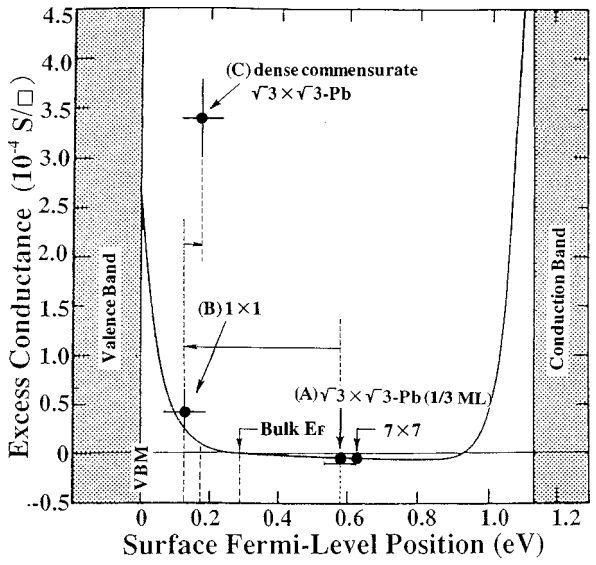

FIG. 4. Calculated excess conductance through the surface space-charge layer as a function of the surface Fermi-level position referred to the VBM. The mobilities of conduction electrons and holes in the layer were assumed to be equal to those in the bulk crystal. The surface E_F positions at the respective phases were determined by the shifts of the bulk-emission peak in UPS spectra in Fig. 3. The excess conductances of the respective phases with respect to that of the $\sqrt{3}\times\sqrt{3}$-Pb ($\frac{1}{3}$ ML) phase were obtained from the conductance increase shown in Fig. 2, and are plotted at the respective E_F positions.

± 0.08 eV above the VBM, and the Schottky-barrier height of about 1.00 ± 0.08 eV for (B) and (C) phases. These E_F positions thus obtained indicate that the surface space charge under the initial $\sqrt{3}\times\sqrt{3}$-Pb ($\frac{1}{3}$ ML) surface (A) is a depletion layer, as similar to that under the clean 7×7 surface; while the layers beneath the (B) and (C) phases become hole-accumulation layers.

It is worthwhile to point out that there are some similar characters between the dense commensurate $\sqrt{3}\times\sqrt{3}$ and HIC/SIC phases. First, the 1.00 ± 0.08 eV of Schottky-barrier height we obtained for the dense commensurate $\sqrt{3}\times\sqrt{3}$ phase is similar to those for the HIC/SIC phases obtained by ultraviolet photoemission spectroscopy (UPS) (1.04 eV) or x-ray photoemission spectroscopy (XPS) (1.09 eV) by Weitering, Ettema, and Hibma.[15] Second, for the dense commensurate $\sqrt{3}\times\sqrt{3}$ phases, the two surface states situated at 0.8 eV below E_F (indicated by an arrowhead) and at E_F in Fig. 3(C) were also observed in the incommensurate phase in Ref. 15, in which the former one was interpreted as a Si dangling-bond state hybridized with Pb $6p_{x,y}$ orbitals, and the latter one is a surface state for E_F pinning to make a high Schottky barrier.[15] Third, the total Pb coverage for the dense commensurate $\sqrt{3}\times\sqrt{3}$ phase is about 1.0 ML ($\frac{1}{3}$ ML+0.7 ML), which is similar to the saturation coverage for the HIC phase, i.e., 1.2 ML.[8] In this way, similarities in electronic structures and saturation coverages between the dense commensurate $\sqrt{3}\times\sqrt{3}$ phase and the HIC phase would imply a similar atomic arrangement in short range; the dense commensurate $\sqrt{3}\times\sqrt{3}$ phase may also be a close-packed 30° rotated Pb(111) layer on a bulk-terminated Si(111) surface like that at the commensurate domains in the HIC phase.[17]

We now come to a discussion of the conductance change in Fig. 2. There are in general three possible contributions to the electrical conductance near semiconductor surfaces:[12] conductions through the grown metal atomic layers, through the surface space-charge layer in the substrate, and through the surface-state bands. In order to estimate the magnitude of the second type, the conductance through the surface space-charge layer was calculated by solving the Poisson equation,[18] the result of which is shown by a curve in Fig. 4. It shows that the conductance through the surface space-charge layer below the 1×1 surface (B) should increase by about $(3\pm 2)\times 10^{-5} S/\square$ due to excess hole accumulation, compared with that of the $\sqrt{3}\times\sqrt{3}$-Pb surface (A). The error comes mainly from the uncertainty in determining the E_F positions by photoemission. This value seems consistent with our measured increase in conductance, $(4\pm 2)\times 10^{-5} S/\square$, in Fig. 2. Therefore it can be said that the excess electrical conductance for the 1×1 phase is mainly attributed to the surface space-charge layer.

When the 1×1 phase (B) transforms into the dense commensurate $\sqrt{3}\times\sqrt{3}$ phase (C), the UPS results in Fig. 3 show that the surface E_F shifts away from the VBM, or in other words, the surface space-charge layer approaches a depletion-layer condition. So the data point for the phase (C) deviate above the calculated curve in Fig. 4. On the other hand, the surface-state peak at E_F grows, which indicates that the dense commensurate $\sqrt{3}\times\sqrt{3}$ surface (C) has become metallic enough. Thus we have to conclude that the steep increase in conductance observed in Fig. 2 cannot be inter-

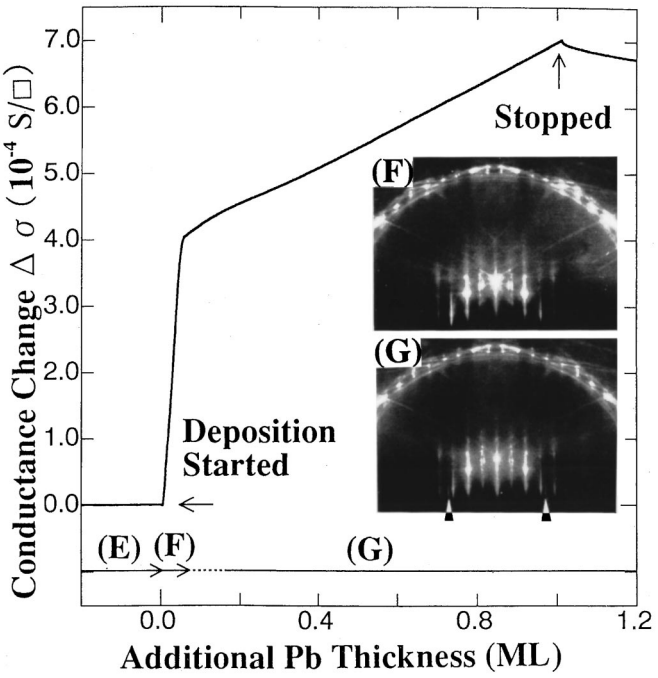

FIG. 5. Change in conductance during additional Pb deposition onto the HIC phase at RT. The RHEED patterns observed in the course of deposition are inserted; (F) the SIC phase, and (G) the SIC phase with Pb islands grown on it. The coverage ranges for the respective RHEED patterns observed are also indicated on the abscissa. The pattern of the initial HIC phase is shown in Fig. 1(E).

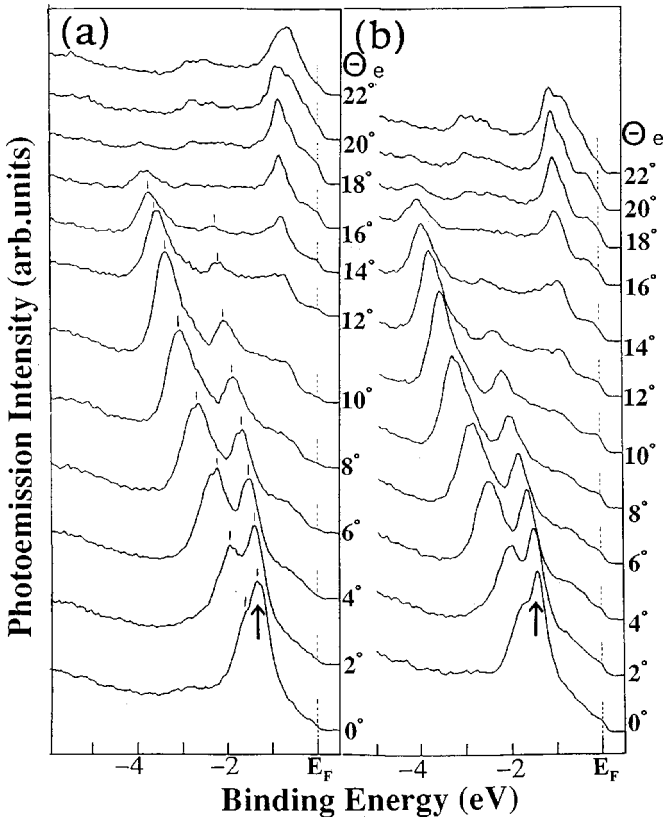

FIG. 6. ARUPS spectra taken from (a) the HIC and (b) SIC phases at RT, respectively. The UV light irradiated the surface with 30° off from the surface normal. The electron detection angle θ_e, indicated on each spectrum, was changed from the surface normal to $[11\bar{2}]$ direction.

preted by the changes of surface space-charge layer, but rather should be attributed to the excess metallic surface state.

Beyond 0.7 ML, Pb crystal islands begin to grow sparsely on the $\sqrt{3}\times\sqrt{3}$ phase as indicated by the RHEED pattern in Fig. 1(D) (in the Stransky-Krastanov growth mode). So the metallic emission at E_F in Fig. 3(D) must partly come from the metallic Pb crystals.

B. On the HIC surface

We carried out similar measurements during additional Pb deposition onto the HIC surface at RT. Figure 5 shows the changes in conductance of the Si wafer and the RHEED pattern observed during a separate deposition under similar conditions. After the evaporator shutter was opened, the surface structure was converted from the HIC phase [Fig. 1(E)] into that shown by a pattern (F) in Fig. 5, accompanied with a steep rise in conductance, up to Pb coverage of around 0.08 ML. Beyond 0.08 ML, the surface structure is further converted into (G) gradually, and the conductance increase turned to be much slower. In pattern (F), a horizontal splitting of the $(\frac{1}{3}, \frac{1}{3})$ streaks can be seen, and the intensity of $(\frac{2}{3}, \frac{2}{3})$ spots are increased. By the scanning tunnel microscope (STM) observations,[8] Seehofer *et al.* find that the commensurate $\sqrt{3}\times\sqrt{3}$ domains are separated by hexagonal domain walls on the surface, Fig. 1(E) (HIC phase), while the commensurate domains are separated by striped domain walls on the surface (F) (SIC phase). In the pattern (G), some Pb crystals are seen to grow on the SIC phase, as indicated by the streaks (pointed by arrowheads) having the Pb lattice constant. These structural changes are in agreement with the phase diagram in Ref. 8.

Figure 6 shows angle-resolved UPS (ARUPS) taken from (a) the HIC and (b) SIC phases. At a glance, the spectra from both phases look very similar to each other. These are also similar to the ones reported by Weitering, Ettema, and Hibma for their incommensurate structure.[15] We should pay attention to two features in the spectra. The first is the emission intensity near E_F; some intensity can be observed at most of the emission angles for both of the HIC and SIC phases. However, by carefully comparing, the intensities at E_F for the SIC (b) are apparently enhanced in most of the emission angles. The second point is the energy positions of the prominent bulk peaks indicated by arrows in the normal-emission spectra, which are found to shift by about 0.54 and 0.44 eV towards E_F for the HIC and SIC phase, respectively, compared with that at the 7×7 surface in Fig. 3. These shifts are similar to the rigid shift in high-resolution Si $2p$ core-level spectroscopy[19] and valence-band spectroscopy[15] for the incommensurate phases. By using the same analysis as in the former section, the surface E_F positions on the respective phases are then estimated to lie at 0.09 ± 0.03 eV and 0.19 ± 0.03 eV above the VBM, which are consistent with our other results measured by Si $2p$ core-level shifts in x-ray photoemission spectra within the experimental errors of ±0.05 eV (the surface E_F lies at 0.13 eV for the HIC, and 0.23 eV for the SIC above the VBM). This means that the

surface space-charge layer below the initial HIC surface is the hole-accumulation layer while it is slightly depleted under the SIC phase.

We now discuss why the SIC phase has the stronger metallic state and the higher electrical conductance than the HIC phase observed in Figs. 5 and 6.

Weitering, Ettema, and Hibma[15] suggest that the metallic surface state in the HIC/SIC originates from the Pb adatoms at the off-centered sites in the commensurate $\sqrt{3}\times\sqrt{3}$ domains. The off-centered-site Pb adatoms make a two-dimensional honeycomb-chained triangular lattice, having an atomic spacing short enough to have large overlap integrals (laterally shorter than in the bulk Pb). On the other hand, according to STM studies,[7,8] the line density of the incommensurate domain walls is 0.13 Å^{-1} for the HIC phase, while it is 0.04 Å^{-1} for the SIC phase, fairly smaller than in the HIC. This means that the areal fraction of the commensurate $\sqrt{3}\times\sqrt{3}$ domains is larger in the SIC phase. Therefore, the density of the metallic surface state will increase with the transition from the HIC to SIC phases. The increased electronic density in this metallic state should contribute to the excess electrical conductance. On the other hand, the conductive electrons in the metallic surface state in the commensurate domains would be scattered by the domain walls. This is revealed by so-called electron standing waves at out-of-phase domain boundaries in STM images.[20] Then, it can be expected that the decrease in the domain-wall density in the SIC phase will lead to an enhancement in the carrier mobility through the metallic surface state.

Because the accumulated holes in the surface space-charge layer below the initial HIC surface are found to be slightly depleted under the SIC surface, the steep increase in electrical conductance observed in Fig. 5 cannot be understood by the band bending. Therefore we have to conclude the enhancement of the metallic surface-state conductance, which is caused by the increased density of electrons therein, and maybe also by enhancement in the carrier mobility, is due to the decrease in carrier scattering at the domain walls.

IV. SUMMARY

We have systematically studied the relation among the changes in surface atomic structures, surface electronic states, and surface electrical conduction during adsorption of additional Pb atoms onto the Si(111)-$\sqrt{3}\times\sqrt{3}$-Pb ($\frac{1}{3}$ ML) surface and the HIC surface at RT. The reasons for the observed conductance changes are explained in terms of the surface-state conduction and the surface-space-charge-layer conduction.

Corresponding to the structural transformation from the $\sqrt{3}\times\sqrt{3}$-Pb ($\frac{1}{3}$ ML) structure to the dense commensurate $\sqrt{3}\times\sqrt{3}$ (1 ML) surface, a newly found phase here, which was formed by additional 0.7 ML Pb adsorption onto the $\sqrt{3}\times\sqrt{3}$-Pb ($\frac{1}{3}$ ML) surface, the surface conductance increased steeply. This change was explained by the two facts that the surface space-charge layer was transformed from a depletion layer to a hole-accumulation layer, and more importantly that the metallic surface state was created. Its atomic structure is suggested to be similar to the commensurate domains in the HIC and SIC phases.

A steep increase in conductance was found also at the transformation from the HIC into the SIC phases with only 0.08 ML Pb additional deposition at RT. This was attributed to the enhancement in carrier concentration through the metallic surface state, but not to the surface space-charge layer below the surface. And we would like to suggest that it is also partly due to enhancement of its carrier mobility, because the domain-wall density is reduced with the transition from the HIC to SIC.

In this way, the dense commensurate $\sqrt{3}\times\sqrt{3}$ phase and SIC phase are found to have the conductive metallic surface states which are considered to originate from the off-centered-site Pb adatoms in the commensurate $\sqrt{3}\times\sqrt{3}$ domains.

ACKNOWLEDGMENTS

We acknowledge Dr. Tadaaki Nagao and Professor Martin Henzler for their valuable discussions. This work has been supported in part by Grants-In-Aid from the Ministry of Education, Science, Culture, and Sports of Japan, especially through Grants-In-Aid for Creative Basic Research (No. 09NP1201) conducted by Professor Katsumichi Yagi of the Tokyo Institute of Technology. We have been supported also by CREST (Core Research for Evolutional Science and Technology) of the Japan Science and Technology Corporation (JST) conducted by Professor Masakazu Aono of Osaka University and RIKEN.

*Author to whom correspondence should be addressed. Present address: Semiconductors Laboratory, The Institute of Physical and Chemical Research (RIKEN), Wako, Saitama, 351-01, Japan. Electronic address: tong@postman.riken.go.jp

[1] C. S. Jiang, S. Hasegawa, and S. Ino, Phys. Rev. B **54**, 10 389 (1996).

[2] X. Tong, S. Hasegawa, and S. Ino, Phys. Rev. B **55**, 1310 (1997).

[3] S. Hasegawa, X. Tong, C.-S. Jiang, and Y. Nakajima, Surf. Sci. **386**, 322 (1997); S. Hasegawa, C.-S. Jiang, Y. Nakajima, T. Nagao, and X. Tong, Surf. Rev. Lett. **5**, 803 (1998).

[4] X. Tong, C.-S. Jiang, and S. Hasegawa, Phys. Rev. B **57**, 9015 (1998).

[5] E. P. Suurmeijer, R. Benedictus, A. van der Stadt, and T. M. Klapwijk, Appl. Surf. Sci. **70/71**, 452 (1993).

[6] G. Quentel, M. Gauch, and A. Degiovanni, Surf. Sci. **193**, 212 (1988).

[7] L. Seehofer, D. Daboul, G. Falkenberg, and R. L. Johnson, Surf. Sci. **307-309**, 689 (1993).

[8] L. Seehofer, G. Falkenberg, D. Daboul, and R. L. Johnson, Phys. Rev. B **51**, 13 503 (1995).

[9] M. Jalochowsky and E. Bauer, Phys. Rev. B **38**, 5272 (1988); Surf. Sci. **213**, 556 (1989).

[10] E. Ganz, I. S. Hwang, F. Xiong, S. K. Theiss, and J. Golovchenko, Surf. Sci. **257**, 259 (1991).

[11] J. A. Carlisle, T. Miller, and T.-C. Chiang, Phys. Rev. B **45**, 3400 (1992).

[12] S. Hasegawa and S. Ino, Int. J. Mod. Phys. B **7**, 3817 (1993); Phys. Rev. Lett. **68**, 1192 (1992); Surf. Sci. **283**, 438 (1993).

[13] H. H. Weitering, D. R. Heslinga, and T. Hibma, Phys. Rev. B **45**, 5991 (1992).

[14] G. V. Hansson and R. I. G. Uhrberg, Surf. Sci. Rep. **9**, 197 (1988); Crit. Rev. Solid State Mater. Sci. **17**, 133 (1991).
[15] H. H. Weitering, A. R. H. F. Ettema, and T. Hibma, Phys. Rev. B **45**, 9126 (1992).
[16] F. J. Himpsel, G. Hollinger, and R. A. Pollack, Phys. Rev. B **28**, 7014 (1983); J. Viernow, M. Henzler, W. L. O'Brien, F. K. Men, F. M. Leibsle, D. Y. Petrovykh, J. L. Lin, and F. J. Himpsel, *ibid.* **57**, 2321 (1998).
[17] F. Grey, R. Feidenhans, M. Nielsen, and R. L. Johnson, J. Phys. (Paris), Colloq. **7**, C-181 (1989); R. Feidenhans, F. Grey, M. Nielsen, and R. L. Johnson, in *Kinetics of Ordering and Growth at Surfaces*, edited by M. Lagally (Plenum, New York, 1990), p. 189.
[18] C. E. Young, J. Appl. Phys. **32**, 329 (1961).
[19] G. Le Lay, K. Hricovini, and J. E. Bonnet, Appl. Surf. Sci. **41/42**, 261 (1991); G. Le Lay, Phys. Scr. **T35**, 25 (1989).
[20] N. Sato, T. Nagao, S. Takeda, and S. Hasegawa, Phys. Rev. B **59**, 2035 (1999).